GAMM-Mitt. **30**, No. 2, 481 – 505 (2007)

On parameter identification for material and microstructural properties

S. Gerlach[*1] and **A. Matzenmiller**[**1]

[1] Institute of Mechanics, University of Kassel
Mönchebergstraße 7, 34109 Kassel, Germany

Received 19 February 2007

Key words identification, inverse problem, optimization, viscoelasticity, micromechanics, composite materials, interphase.

The simulation of the mechanical behaviour of structures with the finite element method is one of the main tasks in engineering mechanics and requires both constitutive and structural parameters. In addition to a qualified geometrical approximation of the structure with the finite element discretization and the definition of initial and boundary conditions it is necessary to select material models for the realistic description of the mechanical system at hand. Furthermore, the material models chosen require reliable numerical data for the associated constitutive parameters, which are usually not known for most new materials like reinforced composites, if their properties are not listed in a database or if they consist of different constituents. Composites usually possess unknown microstructural properties, which cannot be assigned to typical specimen of homogeneous material distribution. Due to the imperfect manufacturing process the mechanical behaviour of composites can significantly vary and the associated material parameters must be determined from the overall behaviour of the composite. Therefore, the unknown material parameters, as the essential input data for the consitutive model for every finite element simulation, must be identified by solving an inverse problem before the complete structure is analyzed.

1 Introduction

The necessity of paramter identification arises in all different fields of engineering science. The unknown parameters may be characteristic moduli of the underlying theory for the material behaviour like the Young's modulus for elasticity, the viscosity for rate dependence or the yield point for plasticity. Due to the progress in material science the determination of model parameters is still an active field of research. Many materials, used nowadays, are often not listed in a database or the material's mechanical behaviour is still not investigated throughly due to the time lagging progress in the development of theoretical models. For sufficiently accurate engineering applications and simulations an adequate constitutive mathematical formulation has to be carefully chosen or developed for the material considered. The mechanical formulation has to describe experimentally all observed material mechanisms like viscoelasticity, rate-dependent plasticity or damage. The unknown material parameters, as the

[*] e-mail: gerlach@ifm.maschinenbau.uni-kassel.de, Phone: +00 49 561 804 2058,
[**] Corresponding author: e-mail: amat@ifm.maschinenbau.uni-kassel.de, Phone: +00 49 561 804 2044,

essential input data for the constitutive model of every finite element simulation, must be identified before the boundary value problem of the complete structure is solved. With increasing complexity of the applied material model the number of its constitutive parameters usually augments and the determination of the parameters raises to a demanding mathematical task.

The scientific literature dealing with different aspects of the identification of material parameters for constitutive equations is quite extensive. An introduction to the experimental determination of material parameters may be found in [1] and a present overview is given by Mahnken in [2]. Examples of use may be found in [3],[4] or [5] for different material models.

The unknown variables of the identification task may also be system parameters like microstructural stiffness properties for the flexible interface in composite materials or nodal stiffness and nodal mass values of the finite element discretization for structures in the context of the model update in vibration analysis [6],[7],[8],[9] or other specific values of systems control theory. See [10] for the basic ideas of system identification in control theory and [11],[12],[13] for examples of application.

The Graduiertenkolleg (graduate college) „Identifikation von Werkstoff- und Systemeigenschaften (Identification of material and system parameters)", sponsored by the Deutsche Forschungsgemeinschaft (German National Science Foundation) from 1993 to 2002 at the University of Kassel, contributed to the progress of this field of research - for details see [14], [15].

The paper starts with a general description of the individual steps for the identification of material and microstructural parameters. The necessary material and microstructural models are given, the basic numerical approach is outlined and some general aspects of the validation and verification of the results are discussed. Two typical examples demonstrate the successful identification of the creep spectrum for the linear viscoelastic material model and the interphase properties of an elastic glass fiber/epoxy resin by means of a micromechanical model.

2 Model equations and identification task

The identification procedure for material or structural parameters consists of three major steps. Experimental investigations are fundamental for this task and must be performed with material specimens or the complete structure. An appropriate testing setup has to be installed in order to provoke the material or structural response to be investigated.

In the next step appropriate model equations possessing free parameters must be developed in order to reproduce the material or structural response experienced from the test at least qualitatively. A number of material models is available on the basis of continuum mechanics to describe the most prominent phenomena of material behaviour encountered, like hysteresis effects under cyclic loading, rate-dependence, or stiffness degradation etc. - see fig. 1. The corresponding theories are classified as elasticity, plasticity, viscoelasticity and viscoplasticitiy according to [16] besides additional models of continuum damage and fracture mechanics.

Heterogeneous materials, e.g. low strength polymers reinforced by stiff glass fibers, may show a very complicated mechanical behaviour on both the phenomenological and the microstructural level. In these cases we resort to a microstructurally based approach to the phenomenological description of the overall material behaviour. By considering the material's

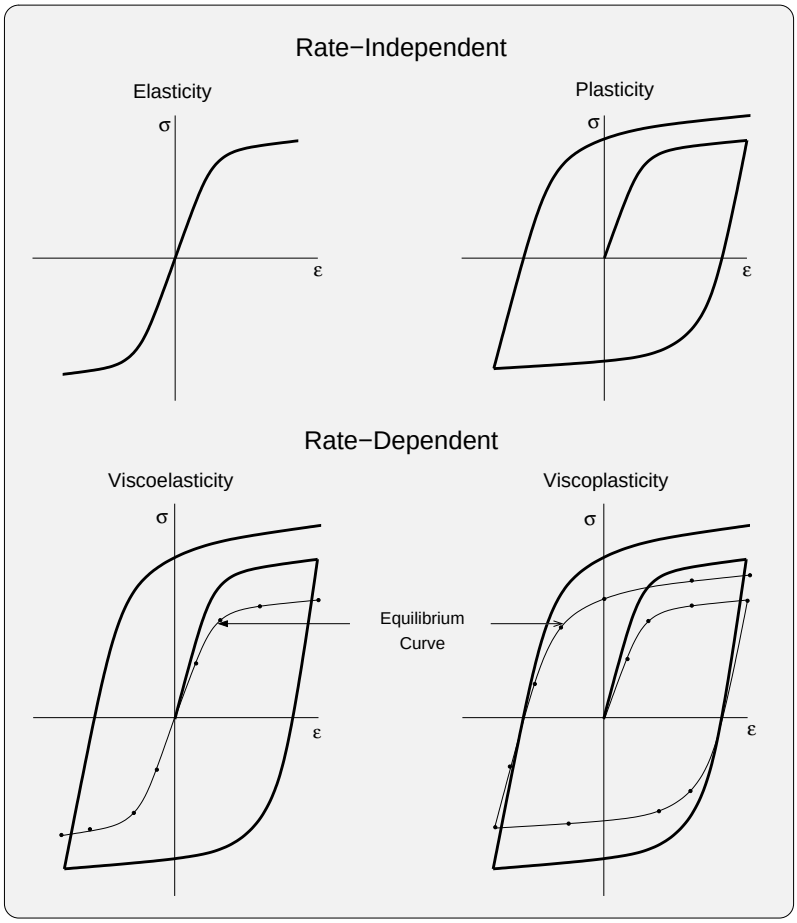

Fig. 1 Classification of material behaviour in [16]

structure on the microscopic level, it is possible to account for the local effects within the individual constituents and interphases of heterogeneous solids and to represent the overall behaviour more accurately with the constitutive model derived. Accordingly, the constitutive relations are set up on the specific microlevel of the material. The model equations for the overall behaviour are formulated by means of a representative volume element (RVE) and the phase properties in order to homogenize the local influences due to the heterogeneous structure of the material - see [17] [18], [19].

The unknown interphase characteristic, which is different from the one of the matrix and the fibers, strongly depends on the material processing with additives or adhesives on the surface of the reinforcing material component. Its parameters cannot be measured directly from tests, but must be rather determined inversely by identifiying the interphase parameters from the material equations of the micromechanical model and the test data from appropriate experiments, as demonstrated in section 5. Knowing all necessary phase and interphase properties,

the constitutive model of the homogenized substitute continuum provides the material equations for the finite element analysis of engineering structures. The two modeling levels of mechanical or building parts, made of composite materials, are shown in fig. 2.

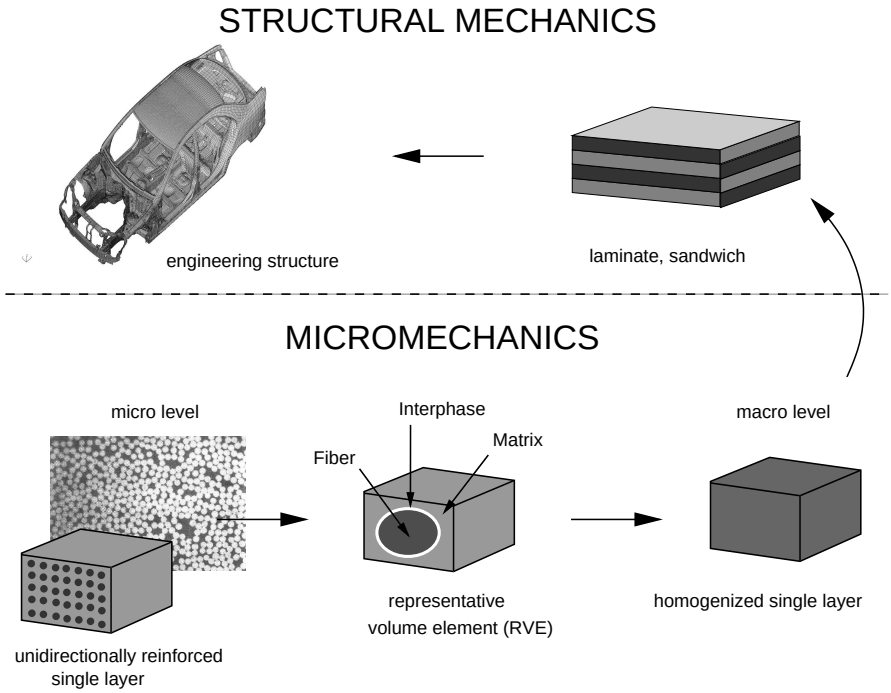

Fig. 2 Modeling levels of structures made of composite materials

3 Parameter identification by nonlinear optimization

Only in very rare cases the material theory chosen will describe the real phenomenological material behaviour exactly. It rather approximates the response of an idealized model based on simplifying assumptions. Therefore, the free parameters $\mathbf{x}$ of the material model are determined such that the model functions $\mathbf{M}(\mathbf{x})$ approximate the test data $\mathbf{d}$ of the material's response best in the sense of some error norm $||\quad||$, usually in the one of the least-square method:

$$f_{\mathsf{LS}}(\mathbf{x}) = \frac{1}{2}||\mathbf{M}(\mathbf{x}) - \mathbf{d}||_2^2 \rightarrow \text{Min.} \tag{1}$$

The quantity $f_{\mathsf{LS}}(\mathbf{x})$, which has to be minimized with respect to the unknown parameter vector $\mathbf{x}$, is called the objective function. In most cases this approach renders a nonlinear optimization problem, the solution vector of which gives the unknown parameters.
Various numerical solution methods for optimization problems are available. One may distinguish between schemes with and without use of gradients of the objective function - see

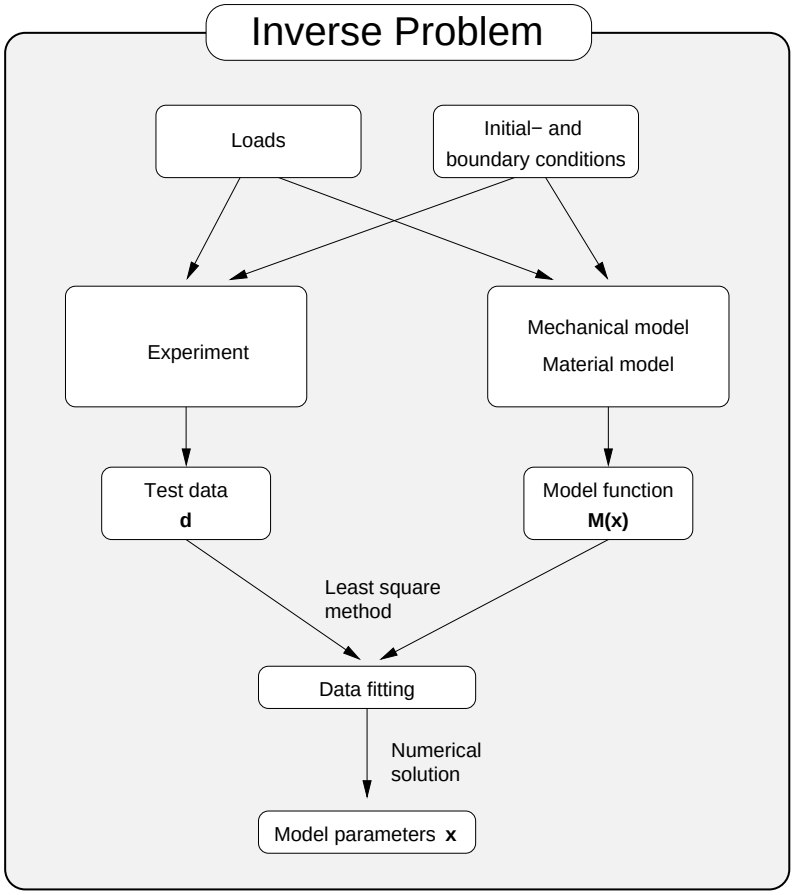

Fig. 3 Schematic illustration of identification procedure

[20]. Gradient-free solution techniques comprise the well-known evolution strategy and the simplex-method, whereas the GAUSS-NEWTON-method or the sequential quadratic programming (SQP) belong to the gradient-based optimization strategies. In this work we focus on gradient-based methods because the objective function of both identification tasks presented can be given in explicit form between the experimental data and the unknown parameters. The objective functions of both examples are differentiable, which is necessary for the applicability of gradient-based methods. The analytical derivation of the gradient of the objective function is an additional step within the identification algorithm which leads to a reduction of computational cost compared to the many function evaluations of gradient-free methods like the evolution strategy in many identification tasks.

The solution methods may also be classified into deterministic and stochastic methods. The objective of stochastic methods is to determine a measure for the uncertainty of the calculated parameters of the underlying model caused by scattering test data. Due to unavoidable systematic inaccuracies of loading, boundary conditions and measurement devices the recorded

test data include errors. Therefore, the sensitivity and the confidence of the calculated parameters represent an important information to the user. The influence of scattering experimental data is not the subject of this paper and the reader is referred to the corresponding literature. A short introduction into different methods for the processing of test data may be found in [21]. The basics of the estimation theory may be found in [22] or [23]. The approximate estimation of the confidence region and the calculation of the correlation coefficients is presented by an example of use in [24] for an elasto-plastic material model, based on the estimation theory. In [25] the identification of the material parameters of a viscoplastic constitutive model is interpreted as a stochastic estimation process. The mean value and the standard deviation of the estimated set of parameters are computed by a statistical analysis which requires a large number of experiments. Therefore, the test data from three types of experiments at different strain rates are completed by artifical data, generated by stochastic simulations, in order to increase the number of input data.

The verification of the algorithm and the validation of the results is an important aspect of every parameter identification. At first the user has to verify that the derivation of the model's equation is accurate as well as the numerical implementation into a computer code is free of errors. Examinations of the plausibility and the application to simulation data should guarantee that the algorithm solves the equations correctly. By inspecting the results of the analysis, the user has to validate that the modeling approach is appropriate to describe the experimentally observed behaviour sufficiently well and that the underlying model equations are the right ones. In the context of the validation process the mechanical meaningful range of the calculated parameters should be given. By means of the limits on the experimental investigations the user has to determine for which loading conditions and load levels the computed values for the parameters hold. It may become necessary that the results from subsequent finite element analysis of engineering structures must be checked for meeting the side-conditions imposed on the identification data.

Some assessment criteria for the interpretation of the results are given in the following. In many cases the unknown parameters represent physical or structural properties, which must belong to a certain interval on the set of real numbers in order to be physically meaningful. For instance, the stiffness parameters or the viscosity coefficients of any material or structure must be non-negative. Therefore, the solution vector is subjected to additional restrictions rendering the identification task to a constrained optimization problem.

The iterative algorithms for the solution of the constrained error functional require starting values, which must be carefully selected in order to achieve convergence to the global minimum of the error norm. Especially, if a multitude of material or microstructural parameters must be identified, there will always be danger that the solution of the iterative scheme depends on the starting vector chosen, since the numerical method may have converged to a local minimum far above the global one. Therefore, additional informations about the order of the unknown parameters may help to choose the initial values in the appropriate range of magnitude at the start of the iterative solution scheme. An obvious strategy for selecting the correct solution from various answers is to run at first a number of iterative approaches with different starting vectors and, thereafter, show that all trials converge to the same result and compute the values of the error norm to pick the solution vector of the lowest one.

Equally important is the analysis of the stability of the final result and the solution method. Identification problems are often ill-posed. That means: Little changes of the experimental data cause large changes of the solution vector for the identified parameters. The mathematical

background of this typical characteristic of inverse problems is given in [26], [27] or [28]. An application-oriented method for the examination of ill-posed problems is discussed in the following section.

4 Identification of creep parameters

Besides the application of general nonlinear optimization algorithms, which can be employed to most identification tasks, it may be more effective to develop a special solution scheme for the specific identification problem at hand. Numerical techniques, tailored towards a particular conceptual formulation, offer some advantages with respect to the stability or the choice of starting values for the iterative solution. An example of this kind is the identification of the viscoelastic line spectrum for a polymer from the experimental creep data, as considered in the following.

4.1 Rheological model

The time-dependent mechanical behaviour of materials shows up in various phenomena. Stress relaxation or creep under constant loading, decay of vibrations or strain and stress rate-dependence are some consequences of viscoelastic material behaviour.
Thus, the constitutive equations, linking the stresses to the strains in the material model, are functions of time. In the case of the infinitesimal strain theory the material behaviour of polymers may be described sufficiently accurate by the theory of linear viscoelasticity. Starting from the Boltzmann superposition principle, the constitutive equations in the linear theory become functionals of the entire preceding stress or strain history:

$$\epsilon(t) = \int_{-\infty}^{t} J(t-\tau)\,\frac{\mathrm{d}\sigma(\tau)}{\mathrm{d}\tau}\,\mathrm{d}\tau \qquad \text{or} \qquad \sigma(t) = \int_{-\infty}^{t} G(t-\tau)\,\frac{\mathrm{d}\epsilon(\tau)}{\mathrm{d}\tau}\,\mathrm{d}\tau, \quad (2)$$

where $\sigma^{,} := \frac{\mathrm{d}\sigma(\tau)}{\mathrm{d}\tau}$ and $\epsilon^{,} := \frac{\mathrm{d}\epsilon(\tau)}{\mathrm{d}\tau}$ are the derivatives of the past stress or strain process with respect to time. $J(t)$ and $G(t)$ are the viscoelastic material functions, representing the temporal behaviour of the material due to the application of a jump in the stress or strain controlled loading history. $J(t) = \epsilon(t)/\sigma_0$ is the creep function and $G(t) = \sigma(t)/\epsilon_0$ the relaxation function. The quantity σ_0 is the normal stress, applied as a jump to the test specimen in the form of the HEAVYSIDE-function. Similarly, the strain ϵ_0 is the magnitude of the jump in the strain-history of the displacement controlled loading on the material. Both kernels, the retardation function $J(t)$ as well as the relaxation function $G(t)$, must be determined from the experimental data. Especially, the relaxation function is needed as the input data for the displacement formulation of the finite element method, if a boundary value problem with a viscoelastic material model must be analyzed in order to solve a design problem in structural engineering. Since only creep data are frequently available from static experiments of specimens under dead loading, an identification procedure is needed to determine the parameters for the retardation function from the given test values. Afterwards the retardation function must be interconverted into the relaxation function for example by means of the LAPLACE transform. An appropriate retardation function will be fitted to the discrete creep data next.
A finite Dirichlet-Prony series is chosen as the characteristic material function, representing

the linear viscoelastic behaviour in most applications well. The retardation function

$$J_{\mathrm{N}}(t) = J_0 + \sum_{k=1}^{N} J_k \left(1 - \mathrm{e}^{-\frac{t}{\tau_k}}\right) \tag{3}$$

corresponds to the generalized rheological model of KELVIN, shown in fig.4.

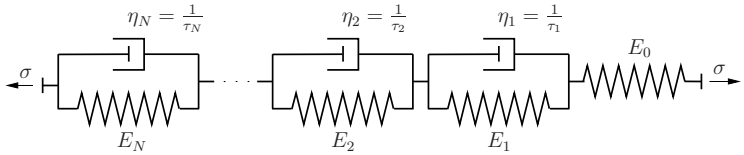

Fig. 4 Generalized rheological model of KELVIN

The unknown parameters J_k and τ_k form the discrete viscoelastic spectrum, as depicted in fig. 5 for a typical linear viscoelastic material.

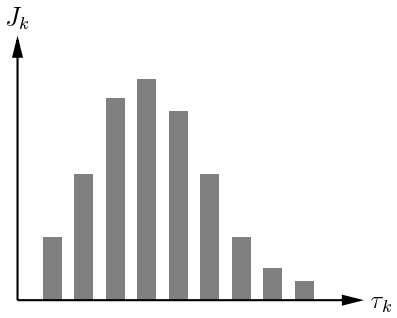

Fig. 5 Illustration of a discrete creep spectrum

The multipliers J_k in front of the exponentials define the spectrum strengths, whereas the quantities τ_k in the denominator of the exponent of the kernel function describe the respondance times. These two parameter sets determine the time-dependent behaviour completely. For a physically realistic material model all of these parameters must be non-negative. Therefore, the fitting algorithm of the material function to the data also has to take into account the constraints:

$$\begin{aligned} J_0 &\geq 0, \\ J_k &\geq 0, \quad \tau_k \geq 0, \quad k = 1, 2, \ldots, N. \end{aligned} \tag{4}$$

4.2 Objective function of the identification task

The identification of the viscoelastic line spectrum from given experimental data requires the solution of an inverse problem. In general, inverse problems have no unique solution, because they are usually ill-posed according to the definitions of HADAMARD - see [29]. Therefore, the objective of the parameter identification is not to determine the exact solution, but to find

the optimal one, minimizing the least square functional f_{LS} or some other norm of the model response $\mathbf{M}(\mathbf{x})$ and the experimental data $\mathbf{d}$, which are both vectors of dimension M in the discrete case.

$$f_{\mathsf{LS}}(\mathbf{x}) = \frac{1}{2}||\mathbf{M}(\mathbf{x}) - \mathbf{d}||_2^2 \rightarrow \text{Min.}, \qquad \mathbf{M}(\mathbf{x}) \in \mathbb{R}^M, \quad \mathbf{x} \in \mathbb{R}^{(2N+1)}, \quad \mathbf{d} \in \mathbb{R}^M \tag{5}$$

The components of the $(2N+1)$-dimensional vector $\mathbf{x}$ comprise the unknown material parameters

$$\mathbf{x}^{\mathsf{T}} = \left[\begin{array}{ccccccc} J_0 & J_1 & \dots & J_N & \tau_1 & \dots & \tau_N \end{array} \right], \tag{6}$$

subjected to the constraints

$$x_i \geq 0, \qquad i = 1, 2, \dots, 2N+1\ . \tag{7}$$

The components of the vector $\mathbf{d}$ contain the values of the experimental creep data at M different points t_j in time.

$$\mathbf{d}^{\mathsf{T}} \;=\; \left[\begin{array}{ccccc} d(t_1) & d(t_2) & d(t_3) & \dots & d(t_M) \end{array} \right] \tag{8}$$

Typically, the number of data points M is much larger than the number of unknowns: $M \gg 2N+1$.

The model response $\mathbf{M}(\mathbf{x})$, given as a function of the unknown parameters $\mathbf{x}$, may be written at the points t_j in time, where the experimental results in eq. (8) are available:

$$\mathbf{M}(\mathbf{x}) = \left[\begin{array}{l} J_0 \; + J_1 \left(1 - e^{-\frac{t_1}{\tau_1}}\right) + \; \cdots \; + J_N \left(1 - e^{-\frac{t_1}{\tau_N}}\right) \\ J_0 \; + J_1 \left(1 - e^{-\frac{t_2}{\tau_1}}\right) + \; \cdots \; + J_N \left(1 - e^{-\frac{t_2}{\tau_N}}\right) \\ \vdots \qquad\qquad \vdots \qquad\qquad \vdots \qquad\qquad \vdots \\ J_0 \; + J_1 \left(1 - e^{-\frac{t_M}{\tau_1}}\right) + \; \cdots \; + J_N \left(1 - e^{-\frac{t_M}{\tau_N}}\right) \end{array} \right]. \tag{9}$$

Various solution strategies have been proposed and published in the literature for the solution of the identification task in eq. (5). The authors investigated four different numerical solution methods and presented the results in [30]. The main features of these methods are shortly repeated in the next subsections and their application to the creep data, found from the experiments of Sarabi in [42], is shown exemplarily.

4.3 Identification strategies without additional informations

The identification of the retardation spectrum without any additional information leads to a general nonlinear optimization problem with non-negative constraints, which must be taken into account by the solution method applied. The discrete least-square approach generates a set of nonlinear normal equations. The iterative solution scheme for the resulting system of nonlinear equations may not converge to the global minimum of the error function for

an arbitrarily chosen starting vector. An example of this kind of problem is the Bertsekas optimization algorithm, a variant of the projected NEWTON method, which iteratively solves the nonlinear optimization task in eq. (5) for a given set of appropriate starting values for the unknown parameters.

$$\mathbf{x}^{(k+1)} = \mathcal{P}\left\{\mathbf{x}^{(k)} - \alpha^{(k)}\mathbf{s}^{(k)}\right\}, \quad k = 0, 1, 2, \ldots \tag{10}$$

$$\mathcal{P}\{\mathbf{x}\}_i := \max(0, x_i^{(k)}), \quad i = 0, 1, \ldots 2N + 1. \tag{11}$$

The operator $\mathcal{P}$ projects those parameters, which violate the constraints in eq. (7), onto the positive range of real numbers. The vector $\mathbf{x}^{(k)}$ represents the parameters of the preceding step or the starting vector $\mathbf{x}^{(0)}$. The parameter $\alpha^{(k)}$ denotes a step-size, chosen by the Goldstein-Armijo descent test. The descent direction $\mathbf{s}^{(k)}$ must be determined in each step by an iteration matrix $\mathbf{B}$ and the gradient $\nabla f(\mathbf{x})$ of eq. (5).

$$\mathbf{s}^{(k)} = \mathbf{B}\,\nabla f(\mathbf{x}) \tag{12}$$

The matrix $\mathbf{B}$ should be positive definite, which is achieved by one of the following choices:

$$\begin{aligned} \text{Gradient method:} \quad & \mathbf{B} = \mathbf{I}, \\ \text{NEWTON method:} \quad & \mathbf{B} = \nabla^2[f(\mathbf{x}^{(k)})]^{-1}, \\ \text{GAUSS-NEWTON method:} \quad & \mathbf{B} = [\mathbf{J}^{\mathsf{T}}\mathbf{J}]^{-1} \end{aligned} \tag{13}$$

with the Jacobian

$$\mathbf{J} = \frac{\mathrm{d}(\mathbf{M}(\mathbf{x}))^{\mathsf{T}}}{\mathrm{d}\mathbf{x}}. \tag{14}$$

In order to ensure a descent at each iteration step of the solution method, an additional condition of the Bertsekas algorithm requires that the matrix has to be 'diagonalized'- see [31] for further explanations.
Alternatively, the authors here developed a different solution strategy, where the identification task is solved in three successive steps - see [32], [33]. At first a qualified tendency function is determined to approximate the test data sufficiently well in time. Such tendency functions are often already available for many materials. By applying the Tschebyscheff-approximation to the tendency function, the respondance times and the spectrum strengths are calculated. In the third step the respondance times from the Tschebyscheff approach are preserved and the spectrum strengths are redetermined by approximating the discrete creep data with an improved choice of the coefficients multiplying the exponentials of the Dirichlet–Prony series. With the given respondance times the determination of the new spectrum strengths leads to a quadratic optimization problem, which may be solved with Wolfe's version of the simplex-method in view of the non-negative constraints on the strength parameters.
Both strategies of this class of identification algorithms have the advantage of not requiring assumptions on appropriate values for the respondance times of the model function in advance as it is the case for the algorithms in the following section.

4.4 Identification with additional information

The general nonlinear identification task can be reduced to a quadratic optimization problem, if the user provides additional informations about the distribution of the respondance times

of the spectrum. The specification of a set of suitable respondance times is a meaningful strategy, as long as an adequate number of respondance times is considered. In this case the experimental data can be approximated with sufficient accuracy, although the set of optimal respondance times for the least error are in general not among the chosen ones. Usually, more respondance times are used as necessary to approximate the experimental data. A large spectrum with many specified respondance times has the advantage of successfully describing the experimental data. However, with respect to the finite element analysis of rate-dependent boundary value problems, a small number of spectrum lines is desirable, since each spectrum line requires the numerical time integration of a convolution integral. For instance not more than ten spectrum lines can be defined in many commercial finite element programs.
Based on a given set of respondance times, various numerical schemes have been developed to determine the corresponding spectrum lines: e.g. the collocation method of Schapery [34], the smoothness constraint approach of Clauser and Knauss [35], the multidata method of Cost and Becker [36] or the enhanced multidata method of Bradshaw and Brinson [37].
The authors applied the windowing-method of Emri and Tschoegl [38], [39], [40] as well as two regularization techniques for the singular values besides the two schemes, outlined already above, in order to identify the viscoelastic line spectrum. However, all of these methods require a careful selection of the respondance times in advance, in order to reduce the identification task to the solution of the linear system of normal equations, as discussed next.
On the assumption that no large differences exist between the strength values of neighboring spectrum lines, the regularization techniques, operating on the singular values, can be used to determine the strength values J_k. The elastic creep compliance J_0 is computed from the first point $t = t_{\mathsf{min}}$ in time of the experimental data. With given values for the respondance times τ_k the least-square problem in eq. (5) simplifies to:

$$f_{\mathsf{LS}}(\mathbf{x}) \quad = \quad \frac{1}{2}||\mathbf{A}\mathbf{x} - \mathbf{d}||_2^2 \rightarrow \text{Min.}, \quad \mathbf{A} \in \mathbb{R}^{M\times N}, \quad \mathbf{x} \in \mathbb{R}^N, \quad \mathbf{d} \in \mathbb{R}^M \tag{15}$$

The objective function is quadratic in the vector $\mathbf{x}$ of the unknown spectrum strengths.

$$\mathbf{x}^{\mathsf{T}} = \left[\begin{array}{cccc} J_1 & J_2 & \dots & J_N \end{array} \right] \tag{16}$$

The vector $\mathbf{d}$ contains the values of the experimental data as in eq. (8). The components of the matrix $\mathbf{A}$ are exponential functions of the chosen respondance times τ_k and the fixed points t_j in time of the experimental data:

$$\mathbf{A} \quad = \quad \left[\begin{array}{cccc} \left(1 - e^{-\frac{t_1}{\tau_1}}\right) & \left(1 - e^{-\frac{t_1}{\tau_2}}\right) & \cdots & \left(1 - e^{-\frac{t_1}{\tau_N}}\right) \\ \left(1 - e^{-\frac{t_2}{\tau_1}}\right) & \left(1 - e^{-\frac{t_2}{\tau_2}}\right) & \cdots & \left(1 - e^{-\frac{t_2}{\tau_N}}\right) \\ \vdots & \vdots & \ddots & \vdots \\ \left(1 - e^{-\frac{t_M}{\tau_1}}\right) & \left(1 - e^{-\frac{t_M}{\tau_2}}\right) & \cdots & \left(1 - e^{-\frac{t_M}{\tau_N}}\right) \end{array} \right]. \tag{17}$$

Obviously, this least-square error functional can be solved with the Bertsekas algorithm also. However, additional insight into the problem is given by the singular values of the matrix $\mathbf{A}$, defined below. Therefore, the least-square expression is solved by means of the singular value

decomposition (SVD) of the matrix $\mathbf{A} \in \mathbb{R}^{M \times N}$, represented by matrix product:

$$\mathbf{A} = \mathbf{V}\,\mathbf{\Sigma}\,\mathbf{U}^{\mathsf{T}} = \sum_{i=1}^{N} \mathbf{u}_i \sigma_i \mathbf{v}_i^{\mathsf{T}}, \tag{18}$$

with the orthonormal matrices of the singular vectors $\mathbf{U} = (\mathbf{u}_1, \ldots, \mathbf{u}_N) \in \mathbb{R}^{N \times N}$ and $\mathbf{V} = (\mathbf{v}_1, \ldots, \mathbf{v}_M) \in \mathbb{R}^{M \times M}$. The diagonal matrix $\mathbf{\Sigma} = \mathrm{diag}(\sigma_1, \ldots, \sigma_N)$ comprises the singular values. By making use of eq. (18), the solution-vector $\mathbf{x}_{\mathsf{LS}}$ of the least-square error functional may be written as:

$$\mathbf{x}_{\mathsf{LS}} = \mathbf{A}^{\dagger}\,\mathbf{y} = \sum_{i=1}^{r} \frac{\mathbf{v}_i^{\mathsf{T}}\mathbf{d}}{\sigma_i}\mathbf{u}_i \tag{19}$$

with r in the upper limit of the sum operator as the rank of the coefficient matrix $\mathbf{A}$: $r = \mathrm{rank}(\mathbf{A})$.

If the matrix $\mathbf{A}$ is invertible ($r = N$), then $\mathbf{A}^{\dagger}$ corresponds to the inverse $\mathbf{A}^{-1}$. Otherwise, the matrix $\mathbf{A}$ is rank deficient ($r < N$), i.e. the number of independent equations is smaller than the number of unknowns. In this case the matrix $\mathbf{A}^{\dagger}$ stands for its pseudo-inverse.

Two characteristic features of the SVD are of interest with respect to the solution of inverse problems [41]: Firstly, the singular values σ_i may be ordered such that they gradually decrease to zero:

$$\sigma_1 \geq \cdots \geq \sigma_N \geq 0 \tag{20}$$

In case the matrix $\mathbf{A}$ is rank deficient ($r < N$), all singular values right of σ_r are zero,

$$\sigma_1 \geq \cdots \geq \sigma_r \geq 0, \qquad \sigma_{r+1} = \sigma_{r+2} = \cdots = \sigma_N = 0, \tag{21}$$

and the numerical schemes, based on a straight forward inversion of $\mathbf{A}$, usually fail. If one or more columns of the matrix $\mathbf{A}$ are nearly a linear combination of the other columns, the matrix is numerically rank deficient. Therefore, particular large differences between successive singular values may occur.

As a second feature of the SVD it is found that the number of sign changes in the components ("waviness") of the singular vectors $\mathbf{u}_i$ and $\mathbf{v}_i$ increases as the index i is enlarged. The series representation of the solution vector $\mathbf{x}_{\mathsf{LS}}$ in (19) shows that the solution is dominated by those singular vectors, which have many sign changes in their components, since their corresponding singular values are small and appear in the denominator. Thus, the uncertainty of the experimental data in the right hand side vector $\mathbf{d}$ is amplified, leading to instabilities of the solution: Small deviations of the experimental data cause large changes of the solution vector as already indicated. This observation is a consequence of ill-posed problems.

The regularization methods approach this undesired phenomenon by introducing filter factors $f(\sigma_i, \alpha)$ as functions of the singular values σ_i and the regularization parameter α. The filter factors shall reduce the influence of those components of the SVD, which are significantly amplified by the reciprocal of the tiny singular values. The regularized least-square solution is given by:

$$\mathbf{x}_{\mathsf{LS}}^{\alpha} = \sum_{i=1}^{N} f(\sigma_i, \alpha) \frac{\mathbf{v}_i^{\mathsf{T}}\mathbf{d}}{\sigma_i}\mathbf{u}_i \tag{22}$$

The most common regularization technique is the truncated singular value decomposition (TSVD), whereby those members of the series representation in eq. (22) are neglected, whose singular values σ_i are smaller than the regularization parameter α. Hence, an obvious filter function is:

$$f(\alpha, \sigma_i) = \begin{cases} 1 & \text{for} \quad \sigma_i \geq \alpha \\ 0 & \text{for} \quad \sigma_i < \alpha \end{cases} \tag{23}$$

According to the idea of the Tikhonov regularization the least-square problem in eq. (15) is replaced by its regularized counterpart

$$\|\mathbf{A}\,\mathbf{x} - \mathbf{d}\|_2 + \alpha^2 \|\mathbf{x}\|_2 \rightarrow \text{Min}, \tag{24}$$

which enforces the solution norm $\|\mathbf{x}\|_2$ to be small in addition to the minimization of the residual norm $\|\mathbf{A}\,\mathbf{x} - \mathbf{d}\|_2$. The regularization parameter α controls the size of the solution norm in the weighted combination of the residual norm $\|\mathbf{A}\,\mathbf{x} - \mathbf{d}\|_2$ and the solution norm $\|\mathbf{x}\|_2$. A large value α favors a small solution norm at the cost of a large residual norm. The resulting filter factor of the Tikhonov regularization becomes:

$$f(\alpha, \sigma_i) = \frac{\sigma_i^2}{\sigma_i^2 + \alpha^2} \tag{25}$$

The choice of the optimal value for the regularization parameter α is the main difficulty in all practical applications. The L-curve criterion of Hansen [41], illustrated in fig. 6, is used here for assistance. Both, the logarithm of the norm of the solution vector $\|\mathbf{x}(\alpha)\|$ of eq. (24) and the logarithm of the defect norm $\|\mathbf{A}\mathbf{x}(\alpha) - \mathbf{y}^\epsilon\|$ are displayed as functions of the regularization parameter α along the axes of the diagram. For discrete ill-posed problems the plot on the log-log-scale of the solution norm versus the residual norm is often L-shaped. The optimal regularization parameter marks the point, where both, the residual and the solution norm, are small.

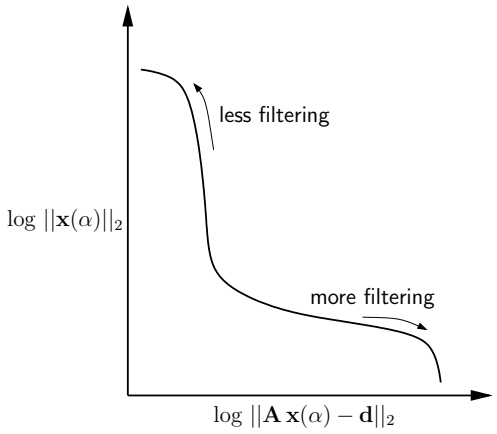

Fig. 6 Plot of solution norm vs. residual norm for L-curve-criterion of [41]

4.5 Comparison of results

The results of four different identification methods are presented together with the experimental data of the creep response for a unidirectional composite, made of glasfiber reinforced polyamide 66 and tested by Sarabi [42]. Fig. 7 shows that all identification schemes provide excellent approximations of the creep data in the time range of the experimental investigation.

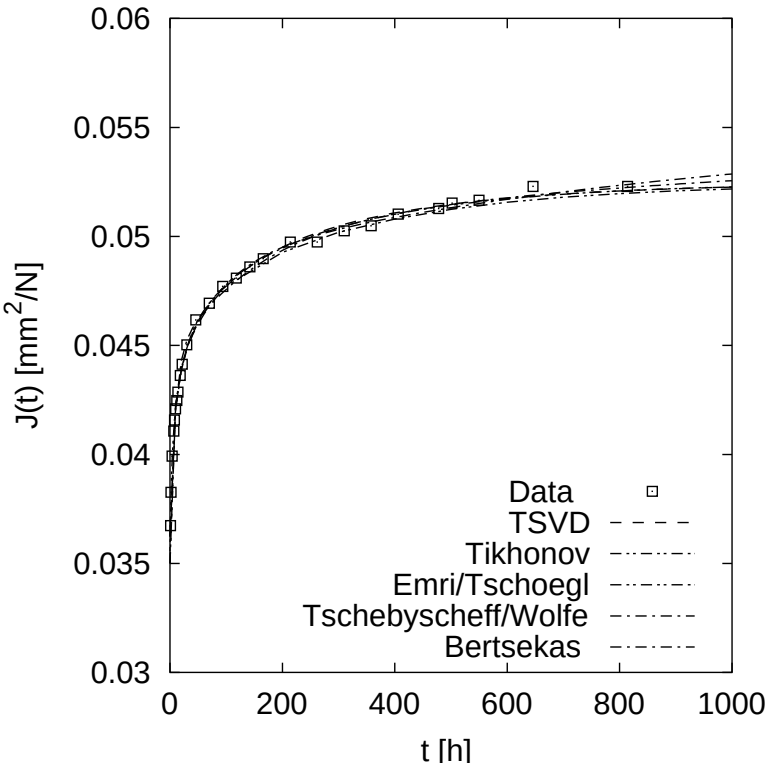

Fig. 7 Various approximations of creep data from [42] on linear time scale

The time interval of the plots for the model different functions, depicted in fig. 8, is extended by an additional decade outside the range of the measured data in the logarithmic representation. The diagram obviously shows the discrepancy between the various creep response functions beyond the last recorded data point in time, although the fit is quite good within that interval of time, where experimental data are available.

Thus, the creep curve should be plotted for each solution of the spectrum and compared to those results, which are gained from the other identification schemes. Special attention must be given to the last data points, indicating whether the creep process tends to its final equilibrium stage, defined by vanishing creep rates.

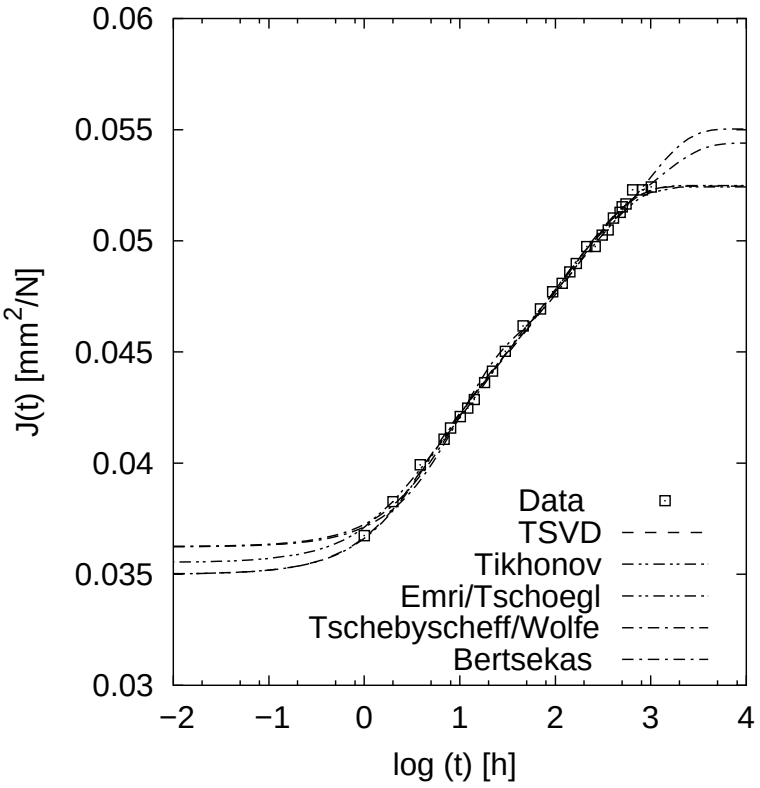

Fig. 8 Approximations of creep data from [42] on logarithmic time scale

4.6 Conclusions for spectrum identification

No additional information about the parameters prior to the identification is required for the straight forward solution of the nonlinear least-square functional with the optimization method of Bertsekas and the Tschebyscheff approximation of an appropriate tendency function with redetermination of the spectrum strengths. Both procedures treat the curve fitting problem of the data with the chosen model function as a purely mathematical one. A disadvantage of these methods is that the convergence of the iterative procedures becomes drastically more difficult with an increasing number of terms in the Dirichlet–Prony series. The algorithms converge to a „stable" minimum of the objective functions for up to four exponential terms. If four or more sum terms are chosen, the starting values must lie in the vicinity of the global minimum of the objective function in order to achieve convergence.

The solution of the objective function with the projected NEWTON method of Bertsekas often depends on the starting values, since the sequence of iteratively computed parameters may converge to a local minimum. In practice the following point of view may be taken: If different starting vectors lead to nearly the same set of solution parameters, the final result represents at least a stable local minimum, which likely is also the global one.

Additional information about the unknown parameters must be provided for the windowing method as well as for the regularization schemes, as the distribution of the respondance times have to be assumed in advance. The set of spectrum lines can be reduced in the case of a qualified estimate of the respondance times. The corresponding class of methods has the advantage of supplying stable results, although the identified parameters may not represent the best mathematical approximation. Though, from an engineering point of view the identified variables represent the ,,better" material parameters, since the discrete viscoelastic line spectrum can be interpreted as an approximation of a continuous spectrum generally. Fig. 9 shows the different line spectra, found out with the various identification methods for Sarabi's experimental creep data in [42].

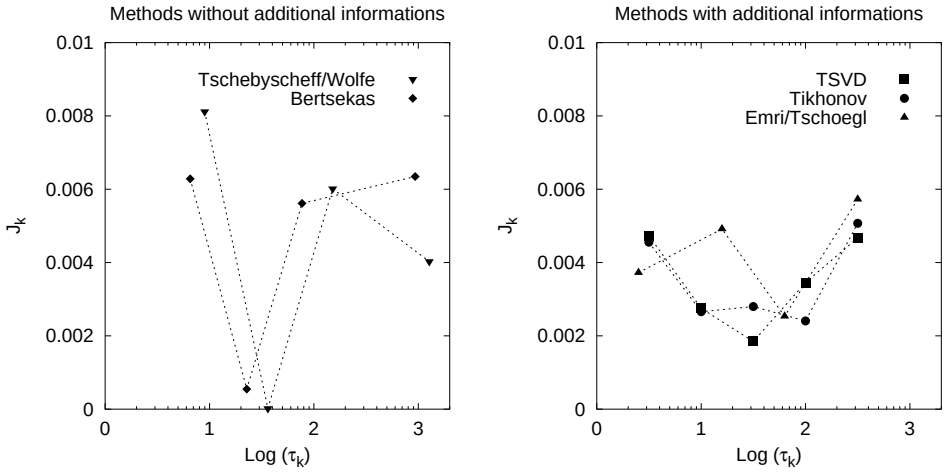

Fig. 9 Identified line spectra of the different identification methods

Although the respondance times are within the same time interval from $0 < \log \tau < 3$, the distributions of the spectrum lines are quite different. The spectra from the methods of the class without additional information show large differences between the neighboring spectrum lines. However, the other class of methods requires additional information, but provides a smoother distribution of the line spectrum.

5 Identification of microstructural properties

The focus is turned next on the identification of microstructural properties for heterogeneous materials, e.g. the stiffness properties of a flexible interphase in a fiber reinforced polymer. The interphase, which is the spatially distributed transition zone around the interface region from the pure filler to the pure reinforcing fiber material, is characterized by graded material properties.

Numerous experimental studies in composite materials research focus on the investigation of the interphase with respect to its influence on the mechanical performance of composite materials, e.g. [43], [44], [45] and [46]. The investigations reveal that the interphase has its own material properties, clearly different from those of the matrix or the fibers, due to coatings

on the fibers or chemical treatment of the fiber surface. The interphase region significantly influences the overall material behaviour of fiber composites as the recorded data of shear and transverse tension tests show. Since the interphase performance depends on the manufacturing process, its characteristics are in-situ properties, which cannot be determined directly from an experiment, performed with specimens, taken from the bulk of the interphase zone. Therefore, the elastic properties of the interphase are identified on the basis of a micromechanical model from the experimental data of the effective elasticity parameters of the homogeneous substitute material.

The search for the missing interphase parameters motivates the development of identification strategies, based on a micromechanical approach with the interphase region as an additional material component with an unknown property. The *Generalized Method of Cells* (GMC), proposed by Paley and Aboudi [47] as an analytical micromechanical approach, is used in this paper as the model to quantify the overall effective properties of the composite with an elastic interphase region of finite thickness. Initially, the micromechanical approach aimed only at the determination of the effective properties for the substitute continuum of a heterogeneous material. However, in [33] an identification procedure is developed, where the in-situ properties of the interphase are determined from the effective properties of the composite and the parameters for the bulk material of the individual phases.

The inverse determination of the interphase properties from the effective material moduli requires the detailed knowledge of the microscopic structure of the composite. The elastic material parameters of the fibers and the matrix as well as the fiber volume fraction and the fiber architecture must be known or assumed in advance. Additionally, the thickness of the interphase region has to be given or estimated. The average properties of the homogenized continuum are related by means of the micromechanical model to the material parameters, the volume fractions and the geometrical arrangement of the individual phases. A third constituent besides the ones for fibers and matrix is introduced in the cells model to account for the interphase in the representative volume element. For a reliable study the effective moduli of the various composite specimens must be measured in experimental testings, in order to account for the different manufacturing influences such as the fiber surface treatment or for additional adhesives. Finally, the model response is fitted best to the experimental data with a gradient-based optimization strategy, requiring the sensitivity analysis of the micromechanical model. With the help of the results of the inverse identification for the interphase properties it is possible to evaluate the mechanical effect of the various manufacturing influences on the interphase characteristics.

5.1 Micromechanical model for composites

The description of the effective (average) behaviour for the equivalent homogeneous comparison material is based on the representative volume element (RVE), whose structure should be typical for the composite, small in comparison to the macrostructure and large with respect to the microstructure. The generalized method of cells has proven to be very efficient in representing the effective elastic and inelastic behaviour of the RVE for unidirectionally fiber-reinforced composite materials - see Aboudi [48]. A two-dimensional variant of it suffices as a model for the composite with continuous fibers in the x_1-direction. The RVE, analyzed with the generalized method of cells (GMC), is given by the unit cell, depicted in fig. 10 (b). It is subdivided into $N_\beta \times N_\gamma$ rectangular subcells with different material properties, which are

specified by the properties of the particular constituents. In the two-dimensional formulation

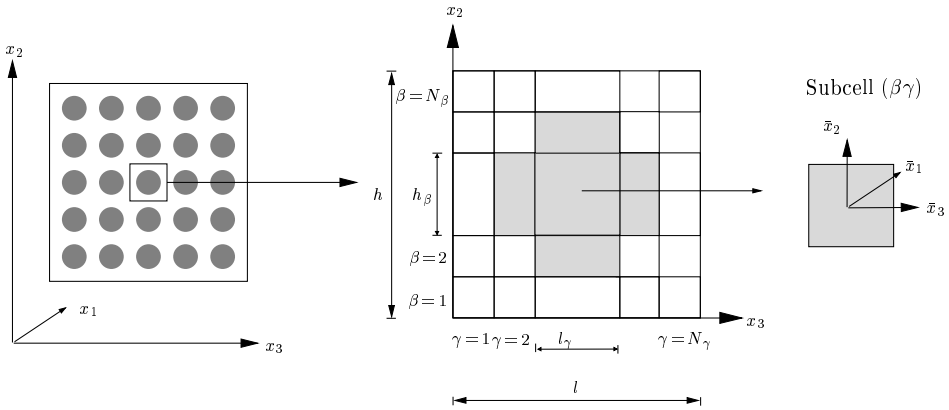

Fig. 10 (a) Composite with double periodic array of fibers in x_1-direction, (b) Representative volume element with subcells and nomenclature

of this analytical model the composite shall consist of continuous fibers in the x_1-direction, which are arranged double periodically in the $x_2 - x_3$-plane - see fig.10a. Due to this assumption it is possible to identify a unit cell as a RVE, which is divided into an arbitrary number of sub-domains, called subcells (fig. 10b) with dimensions h_β and l_γ. For each subcell, subscripted with the indices $(\beta\gamma)$, a bilinear displacement field is assumed and formulated in the local coordinate system. The material behaviour of the cells shall be either isotropic or transversely isotropic. Continuity of the displacements u_i in the local coordinates $\bar{x}_j$ is required at the interfaces between the subcells of the RVEs as well as at the boundaries between adjacent RVEs. The local continuity conditions

$$u_i^{(\beta\gamma)}\Big|_{\bar{x}_2^{(\beta)}=\frac{h_\beta}{2}} = u_i^{(\hat{\beta}\gamma)}\Big|_{\bar{x}_2^{(\hat{\beta})}=\frac{h_{\hat{\beta}}}{2}} \qquad \gamma = 1, 2, 3, \ldots, N_\gamma \tag{26}$$

$$u_i^{(\beta\gamma)}\Big|_{\bar{x}_3^{(\gamma)}=\frac{l_\gamma}{2}} = u_i^{(\beta\hat{\gamma})}\Big|_{\bar{x}_3^{(\hat{\gamma})}=\frac{l_{\hat{\gamma}}}{2}} \qquad \beta = 1, 2, 3, \ldots, N_\beta \tag{27}$$

are relaxed and shall be satisfied only in the average along the plane $\bar{x}_2 = \text{const}$.

$$\int_{-\frac{l_\gamma}{2}}^{\frac{l_\gamma}{2}} u_i^{(\beta\gamma)}\Big|_{\bar{x}_2^{(\beta)}=\frac{h_\beta}{2}} \mathrm{d}\bar{x}_3^{(\gamma)} = \int_{-\frac{l_\gamma}{2}}^{\frac{l_\gamma}{2}} u_i^{(\hat{\beta}\gamma)}\Big|_{\bar{x}_2^{(\hat{\beta})}=\frac{h_{\hat{\beta}}}{2}} \mathrm{d}\bar{x}_3^{(\gamma)} \qquad \gamma = 1, 2 \tag{28}$$

The same procedure is carried out for the second continuity equation along the interface $\bar{x}_3 = \text{const}$. The averaged compatibility equations can be written in matrix form in terms of the phase averaged strains $\langle \boldsymbol{\epsilon}_s \rangle$ and the effective strains $\langle \boldsymbol{\epsilon} \rangle$ of the composite - see Herakovich [49] or Paley et al. [47] for further details.

$$\mathbf{A}_\mathsf{G} \langle \boldsymbol{\epsilon}_s \rangle = \mathbf{J} \langle \boldsymbol{\epsilon} \rangle \; . \tag{29}$$

The coefficients of the matrices $\mathbf{A}_\mathsf{G}$ and $\mathbf{J}$ result from the geometry of the subcells in the RVE. The variable $\langle \boldsymbol{\epsilon}_s \rangle$ is the column vector of the averaged unknown strain components $\langle \boldsymbol{\epsilon}^{(\beta\gamma)} \rangle$ in

the $N_\beta \times N_\gamma$-subcells:

$$\langle \boldsymbol{\epsilon}_s \rangle^{\mathsf{T}} := (\langle \boldsymbol{\epsilon}^{(11)} \rangle, \langle \boldsymbol{\epsilon}^{(12)} \rangle, \ldots, \langle \boldsymbol{\epsilon}^{(N_\beta N_\gamma)} \rangle)^{\mathsf{T}} \tag{30}$$

The averaged strain tensor $\langle \boldsymbol{\epsilon}^{(\beta\gamma)} \rangle$ in the subcell $(\beta\gamma)$ consists of the volume averaged strain components $\langle \epsilon_{ij}^{(i)} \rangle$ in phase (i) filling up the cell.

$$\langle \boldsymbol{\epsilon}^{(\beta\gamma)} \rangle^{\mathsf{T}} := (\langle {\epsilon_{11}}^{(i)} \rangle, \langle {\epsilon_{22}}^{(i)} \rangle, \langle {\epsilon_{33}}^{(i)} \rangle), \langle {\epsilon_{23}}^{(i)} \rangle, \langle {\epsilon_{13}}^{(i)} \rangle, \langle {\epsilon_{12}}^{(i)} \rangle)^{\mathsf{T}} \tag{31}$$

The quantity $\langle \boldsymbol{\epsilon} \rangle$ represents the averaged strain components, written in in vector notation, of the homogenized comparison material.
The equilibrium conditions for the phase averaged stresses $\langle \boldsymbol{\sigma}^{(\beta\gamma)} \rangle$ at the interfaces of the subcells in the RVE

$$\langle \sigma_{j2}^{(\beta\gamma)} \rangle = \langle \sigma_{j2}^{(\hat{\beta}\gamma)} \rangle \tag{32}$$

$$\langle \sigma_{j3}^{(\beta\gamma)} \rangle = \langle \sigma_{j3}^{(\beta\hat{\gamma})} \rangle \tag{33}$$

with $j = 1, 2, 3$; $\beta = 1, \ldots, N_\beta$ and $\gamma = 1, \ldots, N_\gamma$ can be written in matrix form according to Herakovich [49] or Paley et al. [47]:

$$\mathbf{A}_{\mathsf{M}} \langle \boldsymbol{\epsilon}_s \rangle = \mathbf{0} \; . \tag{34}$$

The matrix $\mathbf{A}_{\mathsf{M}}$ contains only known coefficients, depending on the material parameters $C_{ijkl}^{(\beta\gamma)}$ of the constitutive tensor for the constituents. Eqs. (29) and (34) may be combined in the following relationship, written for the tensors between the strains in all subcells $\langle \boldsymbol{\epsilon}_s \rangle$ and the macro strains in the composite $\langle \boldsymbol{\epsilon} \rangle$ in Voigt notation:

$$\begin{matrix} \text{Compatibility conditions} \\ \text{Traction continuity} \end{matrix} \qquad \underbrace{\begin{bmatrix} \mathbf{A}_G(h_\beta, l_\gamma) \\ \mathbf{A}_M(C_{ijkl}^{(\beta\gamma)}) \end{bmatrix}}_{\hat{\mathbf{A}}} \langle \boldsymbol{\epsilon}_s \rangle = \underbrace{\begin{bmatrix} \mathbf{J}(h, l) \\ \mathbf{0} \end{bmatrix}}_{\mathbf{K}} \langle \boldsymbol{\epsilon} \rangle \tag{35}$$

As long as the stiffness coefficients $C_{ijkl}^{(\beta\gamma)}$ and the geometrical dimensions of the subcells are nonzero, the matrix $\hat{\mathbf{A}}$ is non-singular. Therefore, the linear system of equations (35) can be solved uniquely with the matrix $\mathbf{A}$ determined by:

$$\mathbf{A} = \hat{\mathbf{A}}^{-1} \mathbf{K} \tag{36}$$

The matrix $\mathbf{A}$ comprises the elements of the fourth order concentration tensors $\mathbb{A}^{(\beta\gamma)}$ for all subcells assembled in matrix form $\mathbf{A}^{(\beta\gamma)}$:

$$\mathbf{A} = \left[\mathbf{A}^{(11)} \vdots \mathbf{A}^{(21)} \vdots \ldots\ldots \vdots \mathbf{A}^{(\beta\gamma)} \right]^{\mathsf{T}} \qquad \text{with dimensions:} \quad 6 N_\beta N_\gamma \times 6 \; , \tag{37}$$

where N_β and N_γ are the numbers of subcells in x_2- and x_3-direction - see fig. 10 (b).
Finally, the matrix $\mathbf{C}^*$ for the effective stiffness tensor $\mathbb{C}^*$ of the composite is calculated from the matrices $\mathbf{A}^{(\beta\gamma)}$ and $\mathbf{C}^{(\beta\gamma)}$ of the concentration and stiffness tensors of the subcells.

$$\mathbf{C}^* = \frac{1}{hl} \sum_{\beta=1}^{\beta=N_\beta} \sum_{\gamma=1}^{\gamma=N_\gamma} h_\beta l_\gamma \mathbf{C}^{(\beta\gamma)} \mathbf{A}^{(\beta\gamma)} \tag{38}$$

The generalized method of cells allows the modeling of arbitrarily shaped inclusions, embedded in a homogeneous matrix material. Therefore, the interphase region, comprising the material adjacent to the bond, may by taken into account as a thin layer of subcells between the fiber and the matrix phase. The GMC model for the example below consists of 13 by 13 subcells in total as shown in fig. 11 to approximate the microstructure of the composite. The fiber material is surrounded by a thin interphase and embedded into the matrix material. The isotropic material behaviour is described by the bulk and shear moduli K and G

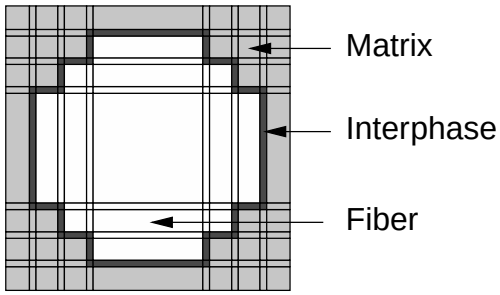

Fig. 11 RVE with interphase (dark cells) modeled by GMC

of the three phases. In order to account for the deviating interphase properties, the authors introduced a scalar κ to relate the isotropic interphase properties $K^{(\mathsf{i})}, G^{(\mathsf{i})}$ to the isotropic elasticity parameters $K^{(\mathsf{m})}, G^{(\mathsf{m})}$ of the matrix:

$$K^{(\mathsf{i})} = \kappa\, K^{(\mathsf{m})}, \qquad G^{(\mathsf{i})} = \kappa\, G^{(\mathsf{m})} \tag{39}$$

5.2 Formulation of identification task

The stiffness properties of the interphase region are found by optimizing the objective function f_{LS} as before in eq. (1) of the least-square error between the data and the model response, which evolves from the underlying micromechanical model. Now the model response $\mathbf{M}(\kappa)$ is a vector-valued function $\mathbf{f}$ of the effective stiffness tensor $\mathbf{C}^*$ as given in eq. (38). It depends implicitly on the unknown interphase scalar κ through the elastic moduli of the cells for the interphase zone according to eq. (39). The parameter κ plays the role of the unknowns $\mathbf{x}$ in eq. (1).

$$\mathbf{M}(\kappa) \;=\; \mathbf{f}\left(\hat{\mathbf{C}}^*(\kappa)\right) \tag{40}$$

Hence, the overall composite stiffness is a function $\mathbf{C}^* = \hat{\mathbf{C}}^*(\kappa)$ of the elastic interphase parameter κ:

$$\mathbf{C}^* = \hat{\mathbf{C}}^*(\kappa) \;=\; \frac{1}{hl} \sum_{\beta=1}^{\beta=N_\beta} \sum_{\gamma=1}^{\gamma=N_\gamma} h_\beta l_\gamma \hat{\mathbf{C}}^{(\beta\gamma)}(\kappa)\, \mathbf{A}^{(\beta\gamma)}(\kappa). \tag{41}$$

Due to the lack of further test data only the effective transverse material stiffness modulus E_{t}^* is chosen as the key quantity for the identification of the interphase properties of the model in this study. The E_{t}^*-modulus of the composite can be expressed by means of the

interconversion rules for the elasticity parameters in terms of the components for the linear elastic, transverse isotropic stiffness tensor $\mathbb{C}^*$, derived from the phase properties by means of the micromechanical model.

$$\begin{aligned} M_1(\kappa) &= E_{\mathsf{t}}^*(\kappa) \\ &= \left\{ \hat{C}_{11}^*(\kappa) \left[\hat{C}_{22}^*(\kappa) + \hat{C}_{23}^*(\kappa) \right] - (\hat{C}_{23}^*(\kappa))^2 \right\} \frac{\hat{C}_{22}^*(\kappa) - \hat{C}_{23}^*(\kappa)}{\hat{C}_{11}^*(\kappa)\hat{C}_{22}^*(\kappa) - (\hat{C}_{12}^*(\kappa))^2} \end{aligned} \tag{42}$$

Note, the parameter κ is determined by fitting the model response best to the experimental data, i.e. minimizing the least-square error functional f_{LS} in eq. (1). Therefore, potential modeling errors or experimental uncertainties like measurement errors or geometrical imperfections are also assigned to this parameter κ.

5.3 Optimization algorithm

The unknown scalar κ is evaluated by solving the nonlinear optimization task with the objective function in eqs. (5) and (42) together with the non-negative constraint: $\kappa \geq 0.0$. The Sequential Quadratic Programming (SQP) of [50] is used here to minimize the objective function. The SQP-method is based on the idea that the given nonlinear optimization task is replaced by a sequence of quadratic subproblems, which can be solved more easily. This solution procedure can be applied, if the number of unknowns at hand is not too large, the function value and the gradient can be computed sufficiently accurate, and if the model response is "smooth" and well-conditioned. The necessary gradient of the function can be determined analytically, i.e. a sensitivity analysis supplies the derivatives of the objective function with respect to the unknown parameter κ. The details are given by the authors in [51].

5.4 Numerical results

The interphase properties are identified using the experimental data of Wacker in [46] and [52] for the transverse elasticity modulus, denoted by $E_{\mathsf{t}}^\star$ for the measured values. In addition Wacker specifies experimentally the elastic material parameters of the fibers and the matrix and gives the fiber volume content $c^{(\mathsf{f})}$, the fiber radius $r^{(\mathsf{f})}$ as well as an estimate for the range of the interphase thickness $t^{(\mathsf{i})}$. All values for the constituents are summarized in table 1.

Material phase	Specific properties		
Glass fiber (E-glass)	$E^{(\mathsf{f})} = 77$ GPa,	$\nu^{(\mathsf{f})} = 0.2$,	$r^{(\mathsf{f})}$=6 μm
Epoxy resin 556/917	$E^{(\mathsf{m})} = 3.11$ GPa,	$\nu^{(\mathsf{m})}$ =0.34	
Interphase thickness	$t^{(\mathsf{i})}$ = 0.3 - 0.7 μm		

Table 1 Properties for material phases of fiber-reinforced composite in [46]

The input data $\mathbf{d}$ for the identification task were provided by the measured values $E_{\mathsf{t}}^\star$ of tension tests on composite specimens transverse to the fiber direction for four different cases of fiber surface treatment, distinguished by the notation: A1128, PU, EP and PE in table 2. The measured values for the effective transverse modulus $E_{\mathsf{t}}^\star$ are listed for each material system in

column three of the same table. The properties of the interphase region in the tests for each set of composite specimens vary due to the different surface treatments and unavoidable material imperfections.

Material	Vol. frac. $c^{(\mathrm{f})}[\%]$	$E_{\mathrm{t}}^{\star}$ [MPa]	Interphase parameter κ $t^{(\mathrm{i})} = 0.3\ \mu$m	$t^{(\mathrm{i})} = 0.4\ \mu$m	$t^{(\mathrm{i})} = 0.7\ \mu m$
556/917 A1128	52.0	11335	- (1.96)	- (1.43)	2.55 (1.20)
556/917 PU	39.3	7193	10.9 (0.78)	3.42 (0.823)	1.72 (0.87)
	43.6	8941	- (2.63)	- (1.94)	4.06 (1.36)
	53.1	12057	- (2.63)	- (1.82)	2.85 (1.33)
556/917 EP	50.7	10269	- (1.14)	5.96 (1.07)	1.92 (0.99)
556/917 PE	46.2	7449	0.76 (0.36)	0.80 (0.42)	0.85 (0.55)

Table 2 Experimental values of $E_{\mathrm{t}}^{\star}$ and identified results κ of interphase parameter for transverse isotropy and in parenthesis for orthotropy

The identified results for the interphase parameter κ are noted in columns four to six of table 2 for three different estimates of the interphase thickness $t^{(\mathrm{i})}$ and for the two assumptions of transverse isotropy and orthotropic material symmetry of the composite lamina. The summary of the results in table 2 shows that the objective function could be solved for an assumed interphase thickness of $t^{(\mathrm{i})}$=0.3 μm only in two cases and for $t^{(\mathrm{i})}$=0.4 μm in three cases, if transverse isotropy is supposed in the GMC-model.

For the case of an assumed interphase thickness $t^{(\mathrm{i})}$=0.7 μm and the supposition of transverse isotropic material symmetry a finite positive value for the parameter κ could be found for all combinations of given fiber volume fraction and surface treatment - see column six of table 2. However, if orthotropic material symmetry is assumed, the scalar κ may be identified for all given thickness values $t^{(i)}$ of the interphase as shown by the results in parenthesis of columns four to six of table 2.

The example shows that the identification procedure works successfully, if the input data allow the solution of eq. (5) in the context of eq. (42). However, not all investigations are satisfactory, since for some sets of input data for the fiber-matrix-interphase system the optimization problem has either no solution or the identified interphase parameter κ is not unique. The vast differences of κ in the case of the small interphases (0.3 μm and 0.4 μm) is apparent, but due to all modeling and numerical errors, approximations and uncertainties of the material data. For example composite materials always include undesirable voids due to inclusions of air pores, which cause deviations of the phase properties in contrast to the material data of the bulk specimen. The spatial discretization of the displacement fields in the micromechanical model introduces unavoidable approximation errors. The least-square method for the computation of the parameter κ fits the model response with all its approximation errors best to the data with their uncertainties. Thus, the optimization task with high sensitivities, as it is the case for thin interphases, may cause dramatic changes of the parameter κ for small variations of the data.

6 Summary

The parameters for the model functions in terms of the retardation spectrum of the linear theory of viscoelasticity and the stiffness properties of a flexible interphase in a composite material have been identified. Different solution methods were discussed for the identification of the discrete viscoelastic line spectrum from a set of experimental creep data. The non-negative constraints to the unknown material parameters are taken into account as an important aspect of the identification task.

The methods presented may be classified into two main groups. The identification algorithms of the first class, the projected NEWTON method of Bertsekas and a combined approach, based on the Tschebyscheff approximation of a tendency function, require no estimates of the unknown creep times. These strategies have the advantage that the user needs no experience with the estimation of the creep times for the nonlinear identification task.

The second class of solution schemes, like the windowing method or the methods based on the regularization of the singular values, requires an assumption about the distribution of the respondance times. Hence, the general nonlinear identification task simplifies to a quadratic optimization problem.

The elastic properties of the interphase region between the fiber and the matrix in unidirectionally reinforced composite materials are identified by means of the generalized method of cells, which allows to approximate an arbitrary geometry of the internal microstructures closely and to determine the overall effective elastic properties of the composite. A numerical identification approach is developed with the help of a gradient-based optimization scheme for the inverse determination of the elastic interphase properties, which are related most simply to the matrix stiffness coefficients. The numerical example demonstrates the successful application of the identification strategy to various sets of test data.

Although the interphase parameters are successfully identified from the experimental data for most composites with various chemical treatment of the fiber surface, the computed results are still not satisfying in all cases. However, the experimental effort is enormously high for providing additional data, e.g. for the effective shear modulus and for the specification of all necessary moduli for the phases and the fiber volume content.

Acknowledgements The authors gratefully acknowledge the financial support of the Deutsche Forschungsgemeinschaft (DFG) through the graduate college ,,Identification of material and system properties".

References

[1] J.F. Bell. *The experimental foundations of solid mechanics*, Mechanics of solids, Springer, Berlin, 1984.

[2] R. Mahnken. Identification of Material Parameter for Constitutive Equations. In *Encyclopedia of Computational Mechanics. Volume 2: Solids and Structures* by E. Stein, R. de Borst and T. Hughes, John Wiley & Sons, 2004.

[3] R. Mahnken and E. Stein. Parameter identification for viscoplastic models based on analytical derivatives of a least-squares functional and stability investigations. *Int. J. Plasticity*, 12(4):451–479, 1996.

[4] R. Kunkel and F.G. Kollmann. Identification of constants of a viscoplastic constitutive model for a single crystal alloy. *Acta Mechanica*, 124:27–45, 1997.
[5] O. Bruhns and D.K. Anding. On the simultaneous estimation of model parameters used in constitutive laws for inelastic material behaviour. *Int. J. Plasticity*, 15(12):1311–1340, 1999.
[6] H. Irretier. *Unbalance Identification of Flexible Rotors based on Experimental Modal Analysis, International Conference on Structural System Identification (COST), Kassel, Germany, 05-07.09.2001. Proc. of the Conf.*, pp. 233-242, 2001.
[7] H. Irretier and S. Lindemann. *Improvement of Damping Parameters of Flexible Rotors by Experimental Modal Analysis and Model Updating, Proc. of the 5th IFToMM Int. Conf. on Rot. Dyn.* 388-395, 2002.
[8] M. Link. *Updating Analytical Models by Using Local and Global Parameters and Relaxed Optimisation Requirements, Mechanical Systems and Signal Processing*, Vol. 12, No. 1, pp. 7-22, 1998.
[9] S. Meyer and M.Link. *Modelling and Updating of Local Non-linearities Using Frequency Response Residuals*. In: Golinval J.-C. and Link M. (Eds.): Mech. Systems & Signal processing, Vol. 17, No. 1, 219-226, 2003.
[10] L. Ljung. *System Identification* In W.S. Levine (eds.): The control handbook, CRC Press, Boca Raton, 1033-1054 , 1996.
[11] H. Hahn, and M. Niebergall. *Development of a measurement robot for identifying all inertia parameters of a rigid body in a single experiment, IEEE Transactions on Control Systems Technology*, Vol. 9, No. 2, pp. 416-423, March 2001.
[12] F. Hecker, and H. Hahn. *Mathematical Modeling and Parameter Identification of a Planar Servo-Pneumatic Test Facility, Part II: Experimental Identification, Nonlinear Dynamics* , Vol. 14, pp. 269-277, 1997.
[13] A. Piepenbrink and H. Hahn. *Fitting mathematical models of a servopneumatic actuator to laboratory experiments by using exact linearisation techniques, Proceedings of the 2nd MATHMOD*, VIENNA, *IMACS Symposium on Mathematical Modelling*, pp. 281-290, Austria, 1997.
[14] P. Haupt, Th. Kersten, and V. Ulbricht, (eds.) *Beiträge zur Modellierung und Identifikation*, Bericht 1/2001 des Instituts für Mechanik, Universität Kassel, 2001. ISBN 3-89792-047-6.
[15] St. Hartmann, P. Haupt, and V. Ulbricht, (eds.) *Modellierung und Identifikation*, Bericht 2/1998 des Instituts für Mechanik, Universität Kassel, 1998. ISBN 3-88122-973-6.
[16] P. Haupt. *Continuum mechanics and theory of materials*. Springer, Berlin, 1. edition, 2000.
[17] S. Nemat-Nasser and M. Hori. *Micromechanics: Overall properties of heterogeneous materials*. Elsevier, Amsterdam, 1. edition, 1993.
[18] J. Aboudi. *Mechanics of composite materials - a unified micromechanical approach*. Elsevier, Amsterdam, 1. edition, 1991.
[19] D. Gross and Th. Seelig. *Bruchmechanik mit einer Einführung in die Mikromechanik*. Springer, Berlin, 3. edition, 2001.
[20] J.E. Dennis and R.B. Schnabel. *Numerical methods for unconstrained optimization and nonlinear equations*. SIAM, Philadelphia, 1996.
[21] V. Blobel and E. Lohrmann. *Statistische und numerische Methoden der Datenanalyse*. Teubner, Stuttgart, 1. edition, 1998.
[22] J.V. Beck and K.J. Arnold. *Parameter estimation in engieering and science*, Wiley, New York, 1977.
[23] H. Schwetlick. Nichtlineare Parameterschätzung: Modelle, Schätzkriterien und numerische Algorithmen. *GAMM-Mitteilungen*, 2:13–51, 1991.
[24] R. Kreißig, U. Benedix, U.-J. Görke. Statistical aspects of the identification of material parameters for elasto-plastic models, *Archive of Applied Mechanics (Ingenieur Archiv)*, Volume 71, Issue 2 - 3, Mar 2001, Pages 123 - 134.
[25] T. Harth, S. Schwan, J. Lehn and F.G. Kollmann. Identification of material parameters for inelastic constitutive models: statistical analysis and design of experiments. *Int. J. Plast.*, 20:1403–1440, 2004.

[26] A.K. Louis. *Inverse und schlecht gestellte Probleme*. Teubner, Stuttgart, 1989.
[27] A.K. Louis. Numerik inverser Probleme. *GAMM-Mitteilungen*, 1:5–27, 1990.
[28] L. v. Wolfersdorf. Inverse und schlecht gestellte Probleme : Eine Einführung. *Sitzungsberichte der Sächsischen Akademie der Wissenschaften zu Leipzig, Mathematisch-Naturwissenschaftliche Klasse*; Bd. 124, H. 5, Berlin : Akad.-Verl., 1994.
[29] J. Hadamard. *Lectures on the cauchy problem in linear partial differential equations*. Yale University Press, New Haven, 1923.
[30] S. Gerlach and A. Matzenmiller. Comparison of numerical methods for identification of viscoelastic line spectra from static test data. *Int. J. Num. Meth. Eng.*, 63: 428–454, 2005.
[31] Dimitri P. Bertsekas. *Constrained Optimization and Lagrange Multiplier Methods*. Academic Press, New York, 1982.
[32] S. Gerlach, A. Matzenmiller, and W. Sippel. Identification of retardation spectra by approximation theory. *Z. Angew. Math. Mech.*, 81:S293–S294, 2001.
[33] S. Gerlach. *Modellbildung und Parameteridentifikation viskoelastischer Faserverbundwerkstoffe*. PhD thesis, Department of Mechanical Engineering, University of Kassel, 2003.
[34] R.A. Schapery. A simple collocation method for fitting viscolelastic models to experimental data. Technical Report 61-23 A, California Institue of Technology, Pasadena, CA, 1961.
[35] J.F. Clauser and W.G. Knauss. On the numerical determination of relaxation and retardation spectra for linearly viscoelastic materials. *Transactions of the society of rheology*, 12(1):143–153, 1968.
[36] T.L. Cost and E.B. Becker. A multidata method of approximate laplace transform inversion. *Int. J. Num. Meth. Eng.*, 2:207–219, 1970.
[37] R. D. Bradshaw and L. C. Brinson. A sign control method for fitting and interconverting material functions for linear viscoelastic solids. *Mech. Time Dep. Matls.*, 1:85–108, 1997.
[38] N.W. Tschoegl and I. Emri. Generating line spectra from experimental response. Part I: Relaxation modulus and creep compliance. *Rheologica Acta*, 32:311–321, 1993.
[39] I. Emri and N.W. Tschoegl. Generating line spectra from experimental response. Part IV: Application to experimental data. *Rheologica Acta*, 33:60–70, 1994.
[40] I. Emri and N.W. Tschoegl. Determination of mechanical spectra from experimental response. *Int. J. Solids Structures*, 32(6/7):817–826, 1995.
[41] P.C. Hansen. *Rank-deficient and discrete ill-posed problems*. SIAM, Philadelphia, 1997.
[42] B. Sarabi. *Das Anstrengungsverhalten von Polymerwerkstoffen infolge ein- und zweiachsigen Kriechens: Ermittlung von Langzeitbemessungskennwerten*. PhD thesis, Department of Mechanical Engineering, Universität Kassel, 1984.
[43] H. Altenbach, J. Altenbach, and R. Rikards. *Einführung in die Mechanik der Laminat- und Sandwichtragwerke*. Deutscher Verlag für Grundstoffindustrie, Stuttgart, 1. edition, 1996.
[44] J.-K: Kim and Y.-W. Mai. *Engineered interface in fiber reinforced composites*. Elsevier, Oxford, 1998.
[45] A. Matzenmiller and S. Gerlach. Micromechanical modeling of viscoelastic composites with compliant fiber-matrix bonding. *Computational Materials Science*, 29(3):283–300, 2004.
[46] G. Wacker. *Experimentell gestützte Identifikation ausgewählter Eigenschaften glasfaserverstärkter Epoxidharze unter Berücksichtigung der Grenzschicht*. PhD thesis, Department of Mechanical Engineering, Universität Kassel, 1996.
[47] M. Paley and J. Aboudi. Micromechanical analysis of composites by the generalized cells method. *Mechanics of Materials*, 14:127–139, 1992.
[48] J. Aboudi. Micromechanical analysis of composites by the method of cells – update. *Applied Mech. Rev.*, 49:83–91, 1996.
[49] C.T. Herakovich. *Mechanics of fibrous composites*. John Wiley & Sons, New York, 1. edition, 1998.
[50] P. Spellucci. DONLP2:SQP/ECQP-method for general continuous non-linear programming. Fortran Routine in http://www.mathematik.tu-darmstadt.de/ags/ag8/Mitglieder/spellucci_de.html, 2000.
[51] A. Matzenmiller and S. Gerlach. Parameter identification of elastic interphase properties in fiber composites. *Composites Part B*, 237: 117–126, 2006.
[52] G. Wacker, A.K. Bledzki, and A. Chate. Effect of interphase on the transverse Young's modulus of glass/epoxy composites. *Composites Part A*, 29A:619–626, 1998.